Transport and metabolism of extracellular free fatty acids in adipose tissue of fed and fasted mice

Murad Ookhtens,[1] Dominic Montisano,[2] Irving Lyon, and Nome Baker

Research Service, Veterans Administration Medical Center, Los Angeles, CA 90073, and Department of Medicine, UCLA School of Medicine, and Crump Institute for Medical Engineering, University of California at Los Angeles, Los Angeles, CA 90024

Abstract We used a new tracer technique, direct tracer injection of [1-^{14}C]palmitate–serum albumin into extracellular fluid (ECF) of epididymal fat pads, to study relative transport rates of ECF-free fatty acids (FFA) to cell-FFA and subsequent esterification to diglyceride fatty acid (DGFA) and triglyceride fatty acid (TGFA) in adipose tissue versus movement of ECF- and cell-FFA into the circulation of mice fed ad libitum or fasted 48 hr. Radioactivity was measured in the following fractions at varying times (for 1 hr): ECF-FFA, cell-FFA, cell-DGFA, cell-TGFA, plasma-FFA (total lipids), and breath CO_2. Pool sizes of ECF-FFA, cell-FFA, cell-TGFA, and plasma-FFA were determined. Analysis by multicompartmental methods (SAAM) indicates that the ECF-FFA compartment of epididymal fat pads is in a relatively rapid exchange with a cellular-FFA compartment, but neither is in direct, nor appreciably rapid, communication with circulating FFA. FFA is rapidly esterified in adipocytes of fed mice, but esterification is significantly inhibited in mice fasted for 48 hr. In both dietary states, essentially all labeled FFA appearing in the circulation was derived from ECF-FFA that were first transferred to the cell, esterified to TGFA, then hydrolyzed to FFA before being transported to the circulation. **—Ookhtens, M., D. Montisano, I. Lyon, and N. Baker.** Transport and metabolism of extracellular free fatty acids in adipose tissue of fed and fasted mice. *J. Lipid Res.* 1987. **28:** 528–539.

Supplementary key words fatty acid transport and metabolism • adipose tissue • free and esterified fatty acids • diacylglycerol • triacylglycerol • plasma free fatty acid transport and oxidation • bicarbonate and CO_2 system • tracer kinetics • multicompartmental analysis • curve fitting • modeling and simulation

Although the heterogeneity of adipose tissue FFA "pools" has been recognized by many investigators (1–4), little is known about the localization and significance of the different pools. In most of the earlier tracer kinetic studies, the adipose tissue-FFA pools have been lumped, for simplicity of analysis and for lack of relevant data, into a single compartment. However, one should at least be able to separate FFA in the extracellular fluid (ECF-FFA) from cell-FFA ["cell-associated-FFA" (5)]. We carried out this separation, coupled with analyses of radioactivity and mass, in various lipid fractions in the cellular and extracellular compartments, including simultaneous measurement of radioactivity in plasma-FFA or -TLFA and in breath CO_2. Thus, it seemed theoretically possible, even in a short-term study, to obtain a great deal of information about the rates of transport and possible pathways of FFA movement into and out of adipocytes in the heterogeneous system that exists in a fat pad.

In the present study we have modified an in vivo technique recently developed in our laboratory (6) to explore these aspects of FFA compartmentalization and transport in the epididymal fat pads of fed and fasted mice. The approach is one in which [1-^{14}C]palmitate, complexed to mouse serum albumin, is injected as a bolus into the fat pad extracellular space in anesthetized animals. Subsequently, we measured the pool sizes of FFA in the extracellular and cell-associated (5) compartments as well as the disappearance of tracer from the ECF-FFA compartment and its appearance in cellular-FFA, -DGFA, and -TGFA as a function of time. In addition, we followed the appearance of tracer in plasma and in breath $^{14}CO_2$ and used these data, together with the measured pool sizes of the total adipose tissue-TGFA compartment, to develop a model of FFA transport and metabolism in which rates of transport in each condition (fed and 48 hr-fasted) were estimated by multicompartmental analysis.

In addition to demonstrating numerous significant changes in various rates of FFA transport into and out of epididymal adipocytes induced by fasting, our analysis demonstrates rather conclusively that FFA molecules in the extracellular compartment into which we injected our

Abbreviations: FA, fatty acid(s); FFA, free fatty acid(s); DGFA, diglyceride fatty acid(s); TGFA, triglyceride fatty acid(s); TLFA, total lipid fatty acid(s); ECF, extracellular fluid; EFP, epididymal fat pad(s).

[1]To whom reprint requests should be directed at: Liver Research Laboratory, VA Wadsworth Medical Center, Bldg. 115, Rm. 316, Los Angeles, CA 90073.

[2]Present address: Department of Medicine, UCSD Medical Center (H 811C), 225 Dickinson Street, San Diego, CA 92103.

tracer have only a very small chance of entering the circulation without prior incorporation into cell-DGFA and cell-TGFA. This was the case even in fasted animals in which net outward transport of FFA is known to be extremely rapid. Apparently the FFA in this extracellular compartment is involved in a rapid cycle of esterification and hydrolysis that includes movement into the cell and back out of the cell before appreciable FFA can escape into the circulation. The activity of this cycle is greatly diminished in fasting, when TGFA synthesis and deposition is slowest.

MATERIALS AND METHODS

Animals and anesthesia

Male Swiss-Webster mice were used. The fed group was kept on Purina laboratory mouse chow and water ad libitum. The body weight of this group on the day of the experiment was 29.3 ± 0.5 g (mean ± SEM, n = 16). The fasted group had access to water, but no food, starting 48 hr prior to the experiment. The body weight of this group dropped by about 23% from a pre-fasting level of 29.6 ± 0.8 g to 22.9 ± 0.6 g (n = 12). On the day of the experiment the EFP of fed and fasted mice weighed (wet) 372 ± 18 (n = 16) and 260 ± 27 mg (n = 12), respectively. Thus, there was a 30% pad wet weight loss due to fasting. The mice were anesthetized with metophane (methoxyflurane; Abbott Laboratories, North Chicago, IL) inhalation before the pads were labeled and they were kept anesthetized throughout the duration of the experiments (60 min).

Tracer and fat pad injection

The isotope was [1-^{14}C]palmitate (58 mCi/mmol, Rosechem, Los Angeles, CA). The details of complexing the tracer FFA to mouse serum albumin have been reported earlier (7). This method yields an FFA-albumin molar ratio of ≃7:1 allowing a maximum of ≃0.4 μCi for a 2-μl bolus injected per fat pad. As before, Evans Blue dye added to the tracer was used as a visual means for quality control of the pad injections (7).

The technique of labeling epididymal and inguinal fat pad lipid-FA by micro-injection of tracer FFA has been developed and extensively validated in our laboratory (ref. 6, and Baker, N., V. Hill, and R. K. Bruckdorfer, unpublished observations). Briefly, it involves gentle externalization of EFP through a small incision in the epididymal region using a saline-wetted Q-tip. With the aid of a magnifying glass loop, a 2-μl bolus injection (≃0.4 μCi) of the tracer FFA is delivered into the ECF of the pad using a 10-μl fixed-needle Hamilton microsyringe. The site of the puncture and injection is closely examined (with the aid of Evans Blue dye) to insure proper delivery of the bolus (7); thereafter, the pad is returned to the abdominal cavity and the incision is clamped off (for zero-time samples the pads are processed, as described below, immediately after the tracer injection). At the appropriate sampling time, the abdomen is opened and the ECF and cells of the pad are separated according to the method described below. To validate the pad injection technique, many tests involving multiple and multisite injections of the boluses in the same pad, distal versus proximal injection of a single bolus and bolus volumes of 2, 5, and 10 μl in different pads were tested. In all cases the disappearance of injected label from pad FFA occurred with $t_{½} \leq 5$ min. The disappearing label was rapidly incorporated into esterified lipid FA, which in the case of fed mice was practically quantitative (≥ 90% of injected dose). The results of our tests indicated that adipocytes in random subportions of the distal and proximal regions of the epididymal (and inguinal) fat pads behave similarly with respect to the kinetics of lipid-FA turnover and metabolism (6). Thus, by tracing fractional changes in a small localized portion of the whole pad, after injection of a single small (2 μl) bolus, we are able to define the fractional rates of FFA turnover and transport for the whole pad. Thereafter, the transport rates (mass fluxes) can be computed using the appropriate lipid-FA pool sizes for the whole pad.

A major assumption that we have made in our modeling efforts was that tracer leaving the ECF compartment was not transported into a fairly stagnant blood pool within the injected fat pad. This was supported by separate unpublished experiments using $^{3}H_2O$ and [^{14}C]glucose and by the data obtained in the present study (see Discussion). Further work is required to determine the effects of varying blood flow rates in fed and fasted states on these transport rates.

Separation of ECF and cells in the fat pad

This technique, which is based upon preliminary observations made in an earlier study (6), involves the rinsing out of the ECF from the EFP by injection of ice-cold 0.9% saline into the extracellular space of the pad. The fat pad of the anesthetized animal is gently exteriorized through the incision site (7) and the rinsing is done by multiple injections of the saline with a 25-gauge needle into the fat pad. After the initial swelling of the sac that encapsulates the pad, it is ruptured by cutting it in several places and the fluid (ECF + saline) is allowed to drain into test tubes. Post-rupture, additional saline rinses can be given; however, the cumulative recovery of ECF-FFA at zero time follows a rise function (discussed below) that is characterized by successively decreasing recoveries, such that a tradeoff is established between the cumulative recovery and the number of rinses. To verify the validity of this technique and to optimize its quantitative yield (within the constraints of the tradeoff discussed), we proceeded as follows. Pads from fed and fasted mice of the

same age and weight group as those used in our tracer-kinetic studies were externalized and injected with 2-μl boluses of [1-^{14}C]palmitate–serum albumin complex, as described above. Immediately after injection of the tracer, each pad was injected with 1 ml of ice-cold saline which caused it to swell as described previously (6). The surface of the swollen capsule was then cut in several places and the ECF + saline was drained into a test tube containing the Bligh and Dyer extraction solvents (7, 8). Four more successive rinses of the ECF space of the pads were given with 1 ml of ice-cold saline and each rinse was extracted for lipids separately. (Note: Until the end of the final rinse, both here and later as presented in the Results, blood and nerve supplies to the tissue were left intact, until final excision of the pad for lipid-FA extraction.) The results showed that the cumulative recovery of the injected labeled FFA as a function of n, the number of 1-ml saline rinses, could be fitted accurately (not shown) by the following equation: cumulative % dose recovered = $80(1 - e^{-0.6n})$. This outcome indicated that when the number of successive rinses was extrapolated to infinity, a maximum of no more than 80% of the injected radioactivity could be recovered in the combined washings by this technique; the rest became tightly bound to, or was taken up by the cells during the rinsing steps. With n = 5 successive rinses, including the initial 1-ml wash used to swell the pad, at least 75% of the injected dose (or $\simeq$95% of all recoverable radioactivity) was recovered. Since the initial wash of the fat pads followed by two additional rinses (i.e., n = 3) resulted in $\simeq$70% recovery of the injected dose, and only about 10% additional recovery was gained by two more washes, we selected n = 3 as the optimum number of rinses. Thus, we standardized our technique with n = 3 and applied the following corrections to the ECF and cell data obtained in the experiments. Since recoveries of the ECF-FFA, based on the above estimates, were about 70%, the actual value of the ECF-FFA was calculated by multiplying the measured value by a factor of 1.4 (= 1/0.7), and cell-FFA was corrected by subtracting 0.3 × (corrected ECF-FFA) from it. In all cases, the sum of the recovered FFA counts in the ECF and cells was practically equal to the injected dose, indicating that the loss of FFA counts during the manipulations for separating the ECF- and cell-FFA pools was negligible.

Lipid extractions and analyses

Lipids were extracted by the method of Bligh and Dyer (8) as described previously (7). As before (7), any sample to be extracted was immediately added to tared tubes containing the extraction solvents, to facilitate the rapid measurement of its weight. Tissue samples were quickly homogenized using a Polytron (model PCU-2-110, Brinkman Instruments) tissue homogenizer. ECF (+ saline rinses) and plasma samples were extracted by vigorous vortexing with the solvents. After separation of phases, aliquots were taken for chemical measurement of FFA pool sizes (9), gravimetric measurement of TGFA ($\simeq$TLFA) pool sizes, and measurements of FFA, DGFA, and TGFA radioactivities by thin-layer chromatography. The latter was done using Redi-Coat-2D plates (Supelco, Inc., Bellefonte, PA) developed in petroleum ether–ethyl ether–glacial acetic acid 50:50:1 (vol/vol/vol). Doses were assayed by extractions in the presence of comparable amounts of unlabeled fat tissue.

Breath $^{14}CO_2$ analyses

A separate group of fed and fasted mice was taken from the same population used for the rest of our kinetic studies to measure the breath $^{14}CO_2$. The method used to trap and assay breath $^{14}CO_2$ was the one we have described previously (10).

Multicompartmental analyses

The tracer data from both fed and fasted mice were fitted with a uniform model that was developed as described in the Results. The SAAM program (11) was used on the IBM 3033 computer at UCLA's Office of Academic Computing to fit the models to the data and to estimate the fractional rates. Our goodness of fit criteria consisted of: *a*) the absence of unequivocally systematic deviations of the fits from the data; *b*) minimization of the sum of squared errors (for selection between alternative models); and *c*) obtaining well-defined fractional rates (low standard deviations on estimated rates).

Assumptions and limitations

Our technique for selectively labeling fat pads (6) differs strikingly from those used earlier by other investigators; therefore, some discussion of the underlying assumptions and limitations may be helpful. The most significant assumption underlying our technique is that labeling of a small localized area of the epididymal fat pad will adequately trace the turnover and transport of lipid-FA in the whole pad. We tried to validate this assumption as carefully and extensively as possible. As noted above, our tests support the premise that the adipocytes in the proximal and distal parts of the epididymal fat pad in mice behave similarly with respect to the kinetics of lipid-FA turnover and transport (see Tracer and fat pad injection, above).

We also assume that there has been no major disruption of cells or redistribution of FFA from the cellular to the extracellular compartment. The first of these assumptions is supported by electron micrographic evidence (6); however, we cannot rule out subtle damage to some of the cells. Certainly, the injection of a small bolus of tracer in saline causes some localized swelling in the region of the fat pad in which the tracer and tracee are undergoing metabolic changes. Whether this swelling causes a redistribution of FFA among the compartments is not known.

We have minimized the volume of the bolus injected (2 μl) to reduce any adverse effects that might arise from the method of tracer delivery. Our earlier studies had shown that bolus volumes of 2, 5, and 10 μl result in identical kinetics of labeled FFA disappearance; thus, it seems fairly unlikely that artifacts strictly related to changes in the ECF volume were present. We think that the initial distribution of the injected tracer closely represents that of the ECF compartment in vivo. Throughout the length of the experiments with fed mice, and up to at least 5 min after injection of the tracer in the fasted mice, the total number of labeled FFA counts injected is accounted for in the TLFA of the pads (see Fig. 1). Thus, the counts disappearing from the ECF-FFA were almost quantitatively recovered in the cell-FFA, cell-DGFA, and cell-TGFA fractions. We had previously verified that the incorporation of the label into the pad phospholipid fraction is practically negligible (12).

We have also tried to assess whether any exit of FFA from the cell into the ECF occurs during our rinsing of the pads for ECF and cell separations. This was done by fixing the cells with cold glutaraldehyde-buffer injection. We found no differences between the results from fixed and unfixed tissues (Baker, N., et al., unpublished observations). However, the possibility of FFA loss from the fixed tissue cannot be ruled out unequivocally and, thus, the possible impact of this limitation on our technique remains unresolved.

Finally, we are working with anesthetized mice that have had surgery (minor), have had a selected fat pad manipulated (gently) and injected. Each and all of these operations could alter the rates of FFA transport and the measured and calculated pool sizes. Therefore, any conclusions that we draw with respect to differences between transport rates in the fat pads of fed and fasted mice apply only to the conditions that we used in our experiments and should not be extrapolated without further experimentation to the unanesthetized normal mouse.

RESULTS

Disappearance of ^{14}C-labeled FA from ECF-FFA of fat pads and appearance in cell nonesterified and esterified lipid fractions

Fig. 1 shows the tracer data defining the disappearance of ^{14}C label from ECF-FFA and appearance in cell-FFA, -DGFA, and -TGFA for mice fed (A) or fasted 48 hr (B). The TLFA radioactivity, shown for both sets of data, depicts the striking difference between the fed and fasted groups; while there is virtually no measurable loss of ^{14}C-labeled TLFA from the pads of fed mice (Fig. 1A), almost half of the corresponding radioactivity is lost from the pads of fasted mice. This outcome is not surprising since the fasting mice are actively mobilizing fat to supply their metabolic energy demands. Thus, all fat stores would be expected to be in a state of lipolysis and net fat contribution to the rest of the organism.

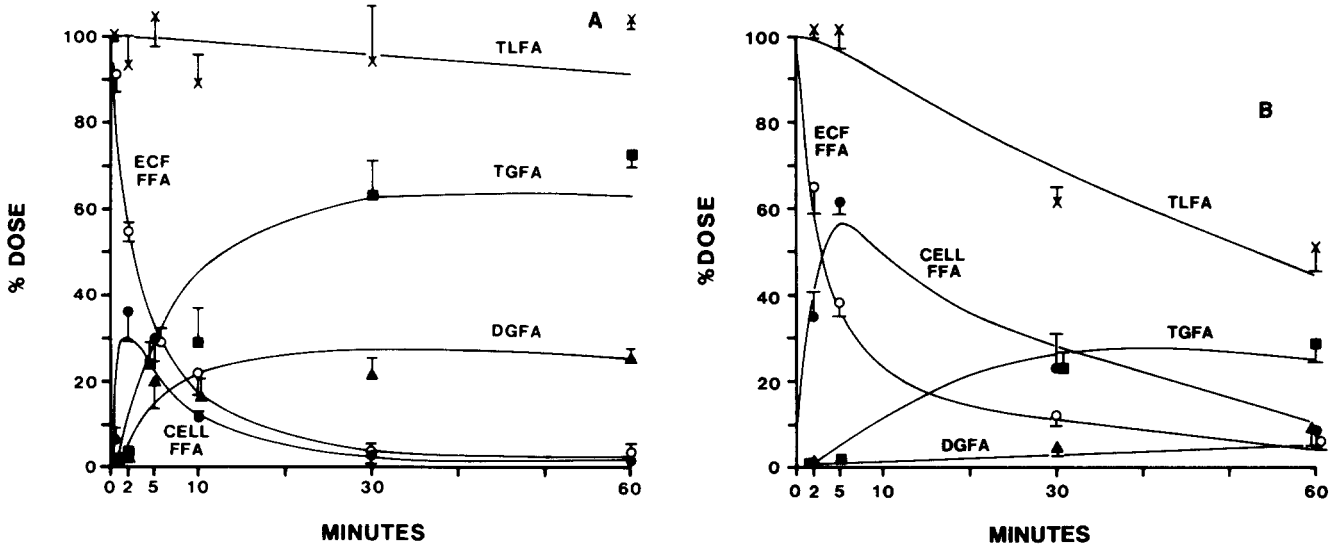

Fig. 1. Tracer data showing the disappearance of the injected labeled dose of [1-^{14}C]palmitate–mouse serum albumin complex from the ECF-FFA of epididymal fat pads of mice fed (A) or fasted 48 hr (B), and appearance into cell-FFA, -DGFA and -TGFA. The sums of all fractions were added to obtain the TLFA data shown. Data points indicate means ± SEM, n = 3 or 4 mice. The curves drawn through the data points represent the fits obtained by using the multicompartmental model shown in Fig. 4 and the SAAM program (11). The values of the fractional rates estimated are presented in Table 1.

There are several other noteworthy features of the tracer data presented in Fig. 1 that merit attention. First, the disappearance of the label from ECF-FFA is faster in the pads of fed mice, resulting in higher levels of labeled ECF-FFA remaining in the pads of fasted mice. Second, the label moves out of the cell-FFA pool at a faster fractional rate in the pads of fed versus fasted mice. This causes the t_{max} of cell-FFA radioactivity to occur earlier and have a smaller peak value than in the fasted mice. Third, as would be expected, there is a consistent trend for higher incorporation of label in the DGFA and TGFA pools of pads from fed as compared to the fasted mice.

The curves drawn through the data points in Fig. 1 represent the fits obtained by using the model (shown in Fig. 4) discussed below.

Appearance of ^{14}C label in plasma-TLFA and breath CO_2

Fig. 2 presents the data for plasma ^{14}C-labeled TLFA (= ^{14}C-labeled FFA) obtained from the same group of fed (A) and fasted (B) mice in which the EFP were labeled. As is evident, much less label was present in the plasma ^{14}C-labeled TLFA of fed mice compared to the fasted ones. The continuous curves drawn through the data points represent the fits obtained by the model presented below (shown in Fig. 4). The broken curves are the predicted responses using a conventional model in which fat pad ECF-FFA is assumed to be in direct contact with the plasma-FFA compartment, as discussed below (see also legend to Fig. 2).

Fig. 3 presents the data for breath $^{14}CO_2$ obtained from a separate group of fed (A) and fasted (B) mice, set aside from the same population used for the EFP-FFA turnover studies. As can be seen, about fourfold as much $^{14}CO_2$ was excreted cumulatively by the fasted as compared to the fed mice, consistent with the physiological correlates of energetics in fasting. The continuous curves represent the fits obtained by using the model discussed below (shown in Fig. 4). Again, the broken curves are those predicted on the basis of a conventional model as discussed below (see also legend to Fig. 3).

Multicompartmental modeling and analysis of the tracer data presented in Figs. 1, 2 and 3

The model shown in **Fig. 4** was selected on the basis of known metabolic pathways and our self-imposed constraint that the whole data set from both fed and fasted groups be fitted with a uniform model. Initially, a conventional model (13, 14) was used in which the plasma-FFA and ECF-FFA compartments were assumed to be capable of directly exchanging FFA molecules, with the net FFA movement being the opposite in fed versus fasted states. However, as noted below, the data were clearly incompatible with this model. The main features of our model are discussed below.

The subsystem defining the epididymal fat pad lipid-FA pools is shown by compartments 1 through 4 (solid circles) and compartment 10 (broken circle). This part of the model is an extension of our previously developed model for lipid-FA turnover in epididymal fat pads of mice (7), in which ECF- and cell-FFA compartments had not been studied separately, but, rather, in a lumped manner for the whole pad. Thus, our present technique of separating the ECF- and cell-FFA compartments allowed us to refine the previous lipid-FA turnover model for the epididymal fat pads to the one depicted here. As in an earlier study (7), the kinetics of the turnover of the

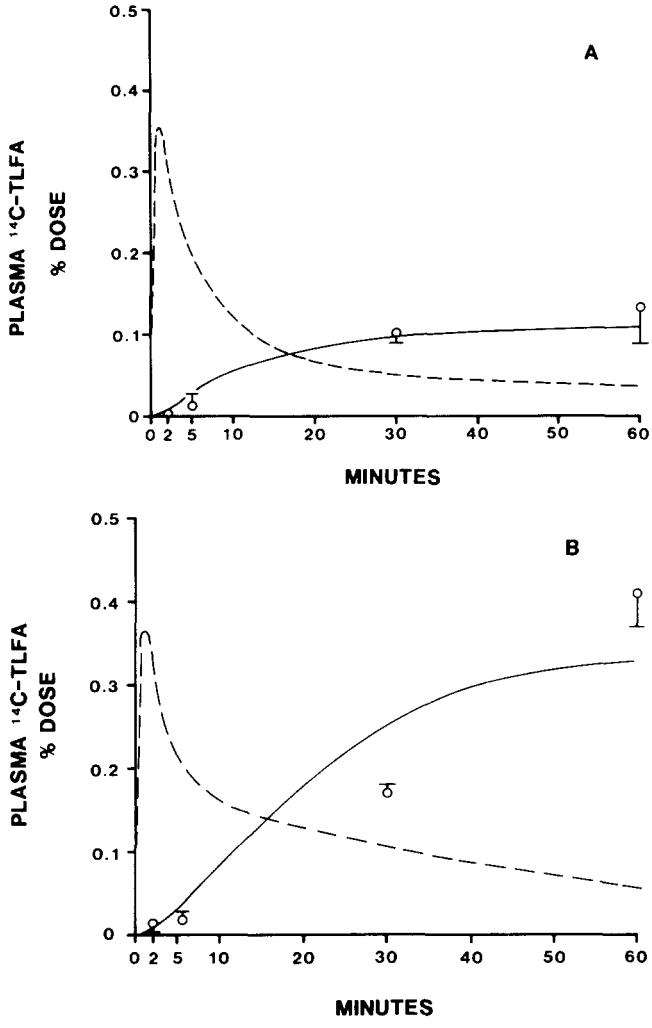

Fig. 2. Appearance of plasma ^{14}C-labeled TLFA (= ^{14}C-labeled FFA) following the injection of labeled FFA-albumin complex into the ECF of epididymal fat pads of mice fed (A) or fasted 48 hr (B). The data points represent mean ± SEM, n = 3 or 4 mice. The continuous curves represent the fits obtained by using the model shown in Fig. 4. See Table 1 for the estimated values of the parameters. Broken curves represent the "best" possible fits when no contribution to the plasma-FFA was allowed to occur from the cell-TGFA pool (compartment 4, Fig. 4; see text).

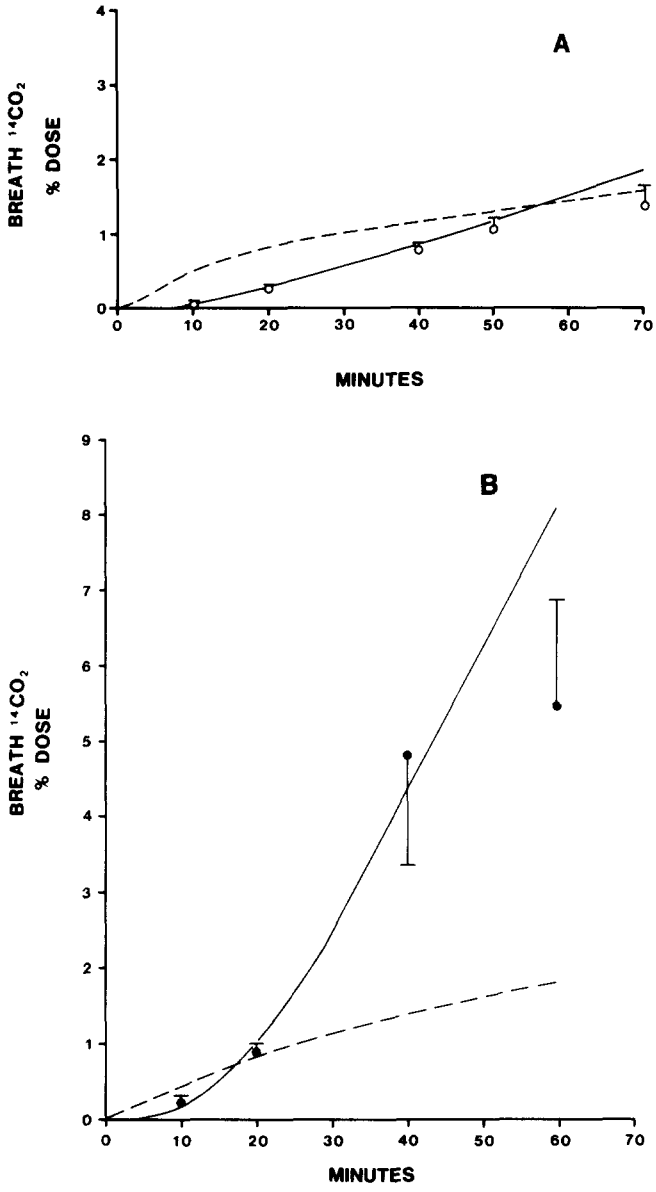

Fig. 3. Cumulative appearance of breath $^{14}CO_2$ following the injection of labeled FFA-albumin complex into the ECF of epididymal fat pads of mice fed (A) or fasted 48 hr (B). The data points represent mean ± SEM, n = 3 or 4 mice. The continuous curves represent the fits obtained by using the model shown in Fig. 4. See Table 1 for the estimated values of the parameters. Broken curves represent the "best" possible fits when no contribution to the plasma-FFA was allowed to occur from the cell-TGFA pool (compartment 4, Fig. 4; see text).

slower pools of cellular-TGFA and the extent of recycling to cell-FFA and ECF-FFA could not be determined accurately in a study of such short duration (1 hr). The extent to which tracer is incorporated into the slowly turning-over TGFA compartments in that time are unknown and are likely to be low (7, 15); moreover, the time scale needed to study slowly turning-over TGFA compartments is known to be of the order of magnitude of days or weeks in mice (see references in 16). Therefore, the TGFA compartments were lumped into a relatively rapidly turning-over compartment (to account for the rapid uptake of TGFA and the recycling to FFA compartments) and a slowly turning-over compartment, depicted in the model by broken lines (Fig. 4), that would include most of the central lipid droplet-TGFA. Compartment 10 was not included in our model-fitting attempts, but it should be included in studies of longer duration and must be taken into account in order to appreciate the differences between measured and model-estimated TGFA pool sizes (see below).

The subsystem defining plasma-FFA turnover had been studied and modeled extensively in our earlier work (13). This subsystem model is defined by comparments 5 and 6 in our present model (Fig. 4). We fixed the fractional transport rates between these two compartments as well as the total irreversible disposal rate from the plasma-FFA compartment (the sum of the two rates shown leaving compartment 5) to the values defined in our earlier work for fed and fasted mice (13). During our fitting attempts, we allowed only a fraction of the total (fixed) irreversible disposal rate to be adjusted by the SAAM program to fit the breath $^{14}CO_2$ data (i.e., L_{75} was defined as an adjustable parameter). This rate, i.e., L_{75}, represents the portion of the total irreversible disposal rate from the plasma-FFA that is accounted for by oxidation.

The last subsystem model required to complete our model for analyzing the whole tracer-kinetic data set was that defining the kinetics of HCO_3^--CO_2 turnover. We have previously developed this subsystem model (shown by compartments 7 and 8 in Fig. 4) (17) to simulate the movement of the CO_2 appearing in plasma to the breath in mice. Therefore, this subsystem model with the fractional transport rates identified earlier was used in our present model.

All the subsystem models discussed above were integrated as shown in Fig. 4. In addition, a summer, depicted by the triangular component No. 9 in Fig. 4, was added to fit the ^{14}C-labeled TLFA value of the fat pads. The resultant integrated model was fitted to the data presented in Figs. 1 through 3 (fits shown by continuous curves). The estimated fractional rates (min^{-1}) are shown in **Table 1.**

Our modeling was done step-wise in both fed and fasted cases. First, the epididymal fat pad lipid-FA subsystem alone was fitted to the data (i.e., compartments 1, 2, 3, 4, and 9). Thereafter, the outcome of this step provided excellent initial estimates of the turnover rates of this subsystem, which then facilitated our extension of the model by integration of the plasma-FFA and HCO_3^--CO_2 subsystems (i.e., compartments 5, 6, 7, and 8). The following is a summary of the attempts made to arrive at a uniform model that would fit the data sets from both fed

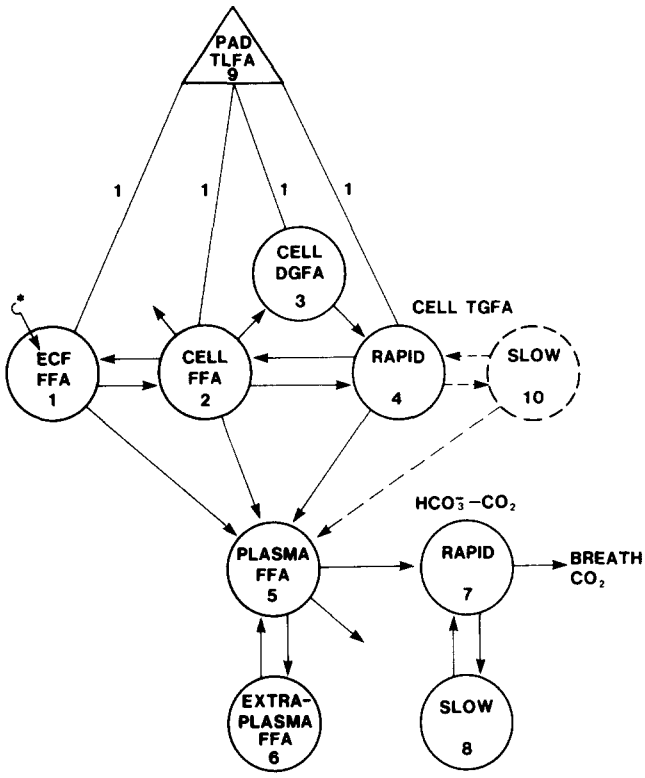

Fig. 4. The integrated multicompartmental model used to fit the data shown in Figs. 1 through 3 (fits represented by the continuous curves drawn on figures). Compartments 1 through 4 define the lipid-FA turnover subsystem in the epididymal fat pad. Compartment 10 represents the slower pools of cell-TGFA (lumped) that do not get labeled appreciably during a 1-hr tracer-kinetic study. Thus, these pools and their contributions to short-term turnover were excluded from our analyses. Compartments 5 and 6 define the plasma-FFA turnover subsystem studied previously (13). Compartments 7 and 8 define the HCO_3^{-1}-CO_2 subsystem studied previously (17). See Results and Discussion for more detailed presentation of other relevant issues and assumptions.

and fasted cases. There was no difficulty involved in fitting the pad lipid-FA subsystem data in either case. As before (7), we did not constrain the relative fluxes of FFA → DGFA → TGFA versus FFA → TGFA to a value of 2 in our model. Theoretically, for the de novo synthesis of every mol of TG (i.e., 3 mol of TGFA) 2 mol of FA from DG should combine with 1 mol of FFA. However, if the DGFA pool were poorly labeled (lower specific activity than the ECF-FFA pool), ratios lower than 2 would be possible. Indeed, the ratios for both fed and fasted groups obtained from the fits were below 2 (fed $\simeq 0.5$, fasted $\simeq 0.1$; computed from values in Table 3 as R_{43}/R_{42}). Our fits resulted in well-defined fractional turnover rates between all four compartments with sharp contrasts between the outcomes of fed versus fasted cases. In the fed case, the small irreversible disposal of the label from the pad lipid-FA pools was found to be from the TGFA compartment (compartment 4, Fig. 4); the irreversible rates leaving the ECF- and cell-FFA compartments were adjusted to zero by the SAAM program (11). In contrast, the large irreversible loss of the label in the fasted case was found to be from the cell-FFA compartment. The question remaining was then to find what fraction, if any, of these irreversible losses was directed toward plasma-FFA and subsequently to breath CO_2.

During the integration of the plasma-FFA and HCO_3^--CO_2 subsystem models, we allowed the putative irreversible loss of lipid-FA from the pad to plasma-FFA to occur from all three major lipid-FA compartments (i.e., 1, 2, and 4). Surprisingly, in neither the fed nor fasted cases were any contributions to the plasma-FFA from pad ECF-FFA and cell-FFA compartments required to fit the data, i.e., whenever these contributions were included, in the presence of the pathway from cell-TGFA to plasma-FFA, they were adjusted to zero by the SAAM program (Table 1). This was to some extent predictable from the delayed appearance of plasma ^{14}C-labeled TLFA and breath $^{14}CO_2$ (see Figs. 2 and 3); however, the results of our modeling provided a rigorous basis for the preclusion of the existence of any direct transport pathways from ECF-FFA and cell-FFA compartments of the fat pads to the plasma-FFA compartment. This is highlighted by the systematically incompatible outcome of trial fits in which the transport of ^{14}C-labeled FA from cell-TGFA (compartment 4) to plasma-FFA was not allowed to take place. Under these conditions the "best" possible fits (by least squares criteria) to the plasma ^{14}C-labeled TLFA and breath $^{14}CO_2$ were those shown by broken curves in Figs. 2 and 3. It is obvious that compatible responses and fits to the data could not be attained with these assumptions. Even when a series of unknown compartments was assumed between the ECF-FFA and plasma-FFA compartments, acceptable fits could not be obtained and, once again, whenever the pathway from cell-TGFA to plasma-FFA was included, the contributions to plasma-FFA from any source other than TGFA were adjusted down to zero. Clearly, the adjustment to zero of the fractional rates of ECF-FFA and cell-FFA transport to plasma-FFA (i.e., L_{51} and L_{52}, respectively) implies that the FA contributed to the plasma from the cell-TGFA does not have to be transported through the cell-FFA and ECF-FFA compartments to reach the plasma. Thus, in both fed and fasted cases, all of the ^{14}C label appearing in plasma-TLFA and breath CO_2 was found to be contributed directly by the rapid cell-TGFA compartment (see Fig. 4 and Table 1). The important implication of this finding is that the ^{14}C-labeled FFA produced from the hydrolysis of cell ^{14}C-labeled TGFA is somehow transported to the plasma without mixing with the cell- or ECF-FFA pools of the pads measured in our present studies. This outcome is consistent with the known heterogeneity of adipose tissue-FFA compartments (1, 18, 19). It implies that the FFA resulting from the hydrolysis of cell-TGFA (by cellular lipases) probably passes through small, localized, and rapidly turning-over

TABLE 1. Effect of fasting on fractional rates (min^{-1}) of FA transport in epididymal fat pads of mice

Fractional Rate[a]	Fed	Fasted 48 hr	P
L_{21}	0.48 ± 0.067[b]	0.30 ± 0.040	< 0.01
L_{12}	0.55 ± 0.20	0.11 ± 0.034	< 0.01
L_{02}	0	0.017 ± 0.0029	< 0.01
L_{42}	0.25 ± 0.021	0.027 ± 0.0054	< 0.01
L_{24}	0.014 ± 0.0047	(0.009)[c]	
L_{32}	0.13 ± 0.016	0.0026 ± 0.0019	< 0.01
L_{43}	0.015 ± 0.0050	0.00035 ± 0.023	n.s.
L_{51}	0	0	
L_{52}	0	0	
L_{54}	0.0035 ± 0.00043	0.019 ± 0.0033	< 0.01
L_{65}	1.61[d]	0.76[d]	
L_{56}	0.050[d]	0.06[d]	
L_{75}	0.37 ± 0.046	0.77 ± 0.12	< 0.01
$L_{05} + L_{75}$	1.47[d]	1.20[d]	
L_{87}	0.085[d]	0.085[d]	
L_{78}	0.0034[d]	0.0034[d]	
L_{07}	0.34[c]	0.34[c]	

Estimates of rates are obtained by fitting the model shown in Fig. 4 to the data shown in Figs. 1 through 3 (fits shown by continuous curves). The SAAM program (11) was used to fit the data and to estimate the fractional rates.

[a]Convention used: L_{ij} defines fractional rate into compartment i from compartment j.

[b]Mean ± SD (n = 3 or 4 in each data set used).

[c]This rate could not be resolved by computer analysis. It tended to be driven to zero by the SAAM program. Instead, it was estimated based on the requirement of near-steady-state conditions for the pool size of cell-FFA during our study. Its value was calculated as the ratio of the transport rate required to maintain this steady-state (i.e., R_{24}, Table 3) to the computed cell-TGFA pool size (Table 2).

[d]These rates were fixed during the fitting process and set equal to those computed in our earlier studies (13, 17).

cell-FFA and ECF-FFA pools before entering plasma-FFA. Thus, the pools of cell-FFA and ECF-FFA involved in the turnover and transport of FFA to the circulation may be kinetically distinct from the ECF-FFA and cell-FFA compartments traced in our studies.

In the fasted case, the major irreversible disposal rate of ^{14}C-labeled FA from the pads was the efflux from the cell-FFA compartment (compartment 2) to an unidentified destination, since none of it could be accommodated by appearance of label in plasma (and thus in breath $^{14}CO_2$). We attempted to fit our data by allowing this large efflux to pass through an unidentified, nonlipid compartment (that would serve as a delay compartment) on its way to the plasma compartment. With this assumption, fits to the data in all compartments were fairly satisfactory, with the exception of the fitted values to the later (30 and 60 min) time points of plasma data which fell drastically short of the measured values. When the single delay compartment discussed above was replaced with a number of compartments in series, or replaced by a pure time delay, no additional improvement took place; in fact, the rate of efflux of cell-FFA through these added components was driven to zero by the SAAM program. In addition, in almost all of the above and in other attempts (not presented here), whenever the transport from cell-TGFA to plasma-FFA was included, all other hypothesized pathways of transport of FA from pad to plasma were driven to zero during the process of fitting. Thus, based on the multicompartmental analysis and fitting, we concluded that, in the fasted state, the unaccounted for loss of radioactivity from the pad at later times was not due to efflux of labeled cellular-FFA either directly or indirectly to plasma-FFA. (Note that, as stated in Materials and Methods, no substantial labeling of phospholipids occurred in our earlier studies (12). Thus, it is highly unlikely that the missing activity could be in that fraction. Furthermore, phospholipids are included in the total lipid extract and would have been accounted for had they been highly labeled. The loss of label by cell rupture also seems unlikely, since such a loss, if it were due to the labeling technique, would have been observed in the fed mice, too.)

Pool sizes and transport rates

The following pool sizes were measured in our studies: ECF-FFA, cell-FFA, cell-TGFA, cell-TLFA, and plasma-FFA (**Table 2**). To compute the transport rates (nmol of FA/min), we made the assumption of near steady-states for the pool sizes during our 1 hr kinetic studies. (Note: our calculations of transport rates are meaningful when there are no other exits or inflows into the system other than those discussed below.)

In the study with fed mice, starting with compartment 1 into which tracer FFA was injected, the transport rate between ECF- and cell-FFA was computed (pool size × fractional rate). Assuming an equal transport rate between ECF- and cell-FFA compartments, the pool size of cell-FFA involved in the kinetic turnover in the course of our study was computed (Table 2). Using the computed pool size for cell-FFA, the transport rates of FA to cell-DGFA and cell-TGFA were computed. In order to maintain the cell-FFA compartment at steady-state, the transport rate of cell-TGFA to cell-FFA was set equal to the sum of the rates leaving the cell-FFA. This allowed computation of the size of the rapid cell-TGFA compartment which, in turn, was used to compute the rate of FA transport to plasma-FFA (i.e., R_{54}). The measured plasma-FFA pool size was used to compute the transport rates between this pool and others. To balance the transport rates so that cell-TGFA and plasma-FFA pools also remain at steady-state, input of unlabeled FA to these two compartments is required. The source of the first one, i.e., the inflow into cell-TGFA, could be de novo lipogenesis of cell-TGFA since the mice were in the fed state. (Note: the inflow of unlabeled FA to compartment 4 is not shown in Fig. 4.) In fact, the lipogenic rate would most likely exceed R_{54}, resulting in a slow accumulation of cell-TGFA over long periods. The source of the second inflow of unlabeled FA, i.e., to plasma-FFA, could be the slowly turning-over and

TABLE 2. Comparison of lipid-FA pool sizes (nmol FA/fat pad) between the fed and fasted groups

Compartment No.[a]	Description	Fed			Fasted 48 hr			P
		Measured	Computed	n	Measured	Computed	n	
1	ECF-FFA	73.4 ± 6.8[b]	73.4	16	95.0 ± 7.3	95.0	12	< 0.05
1	Cell-FFA	323 ± 36.0	64.0	16	739 ± 99.5	259	12	< 0.01
3	Cell-DGFA		555			1,910		
4	Cell-TGFA[c]	(848 ± 64.5) × 10^3	1,740	16	(645 ± 78.1) × 10^3	1,320	12	< 0.05
5	Plasma-FFA[d]	630 ± 47.1	630	16	755 ± 92.6	775	8	n.s.

[a] Compartment numbers correspond to those shown in Fig. 4.
[b] Mean ± SEM.
[c] Estimated from gravimetric measurements by assuming 1 mole of TGFA = 256 g.
[d] Plasma volume (ml) = 5% body weight (g) was used to estimate the plasma-FFA pool sizes for both fed and fasted groups.

large cell-TGFA pool represented by compartment 10. This pool remained practically unlabeled (i.e., it had low specific activity) during our study and could serve as the source of massive inflow of unlabeled FA into plasma-FFA to balance the irreversible disposal of FFA from the latter.

The case of the fasted mice presented additional complications. First, there was the loss from the cell-FFA compartment that could not be accounted for in any compartment or end-product measured. Second, the fractional rate of recycling from the rapid compartment of cell-TGFA to cell-FFA, i.e., L_{24}, could not be estimated accurately from the data of the type and duration that we have obtained (it was driven to zero during SAAM analyses). To overcome these difficulties, an additional assumption had to be made in order to be able to compute the transport rates. This assumption was that of keeping the proportion of the rapid cell-TGFA to the slow cell-TGFA compartments the same as that in the fed state. With this assumption, the transport rates were all computed in the same manner as those in the fed state. All transport rates (nmol FA/min) are shown in **Table 3.**

The only measured pool sizes used in the computation of the transport rates were those of compartments 1 and 5. The rest of the pad lipid-FA pool sizes involved in the kinetic turnover and used for transport rate computations were dictated by the assumption of steady-state conditions. These computed pool sizes are also shown in Table 2. The differences shown in these tables between measured and calculated pool sizes and rates of FFA transport in and out of EFP of fed and fasted mice are discussed below.

DISCUSSION

We have recently described a new approach for studying the esterification of labeled FFA following direct injection of the tracer into the extracellular fluid of selected fat pads (6). Even though we were aware that the tissue-FFA compartments were probably poorly mixed (1-4), our initial approximations of FFA esterification rates were based upon the tentative assumption that the tracer in the ECF-FFA compartment mixed with the cell-FFA pool as though these FFA pools were a single homogeneous compartment (6). Subsequently, using the same direct tracer injection technique in tumor-bearing mice, we found that labeled palmitate does indeed pass from the ECF-FFA compartment through a very large, presumably cell-associated, diluent FFA compartment before it is incorporated into cell-DGFA and -TGFA (7). However, without further fractionation of the compartments, it was not possible to obtain the information that would define some of the more subtle aspects of this potentially complex metabolic system.

Accordingly, we have refined our original technique so that we could characterize in greater detail a number of metabolic pathways traversed by FFA in adipose tissue; namely, the kinetics of fluxes between the intra- and extracellular-FFA and cell-TGFA compartments, the relative rate of ECF-FFA transport directly into plasma-FFA compared to the rate of ECF-FFA uptake by the adipocytes, and the extent to which FFA derived from the hydrolysis of newly labeled cell-TGFA recycled back to the ECF-FFA compartment, or entered the plasma-FFA compartment by other channels. The major modifications that we have made that allowed us to evaluate some of these important quantitative and qualitative aspects of FFA transport from ECF-FFA into cell-FFA (and into FA esters) and into the circulating plasma-FFA compartment in both fed and fasted mice are: the separation and analysis of the ECF- and cell-associated FFA compartments and the simultaneous measurement of radioactivity in both plasma-FFA compartment and breath CO_2, along with the more conventional tissue lipid analyses.

Our results provide strong evidence that FFA molecules that were traced by the direct injection of [1-^{14}C]palmitate into the ECF of epididymal fat pads were preferentially taken up by the adipocytes before they could reach the nearest capillary. Based upon extensive kinetic data analysis which consistently resulted in adjusting to zero the rates of ECF-FFA and cell-FFA transport to plasma-FFA (i.e., L_{51} and L_{52}), we conclude that no appreciable

TABLE 3. Effect of fasting on transport rates (nmol FA/min) of FA in epididymal fat pads of mice

Transport Rate[a]	Fed	Fasted 48 hr	P
R_{21}	35.2 ± 14.0[b]	28.5 ± 8.46	n.s.
R_{12}	35.2 ± 12.8	28.5 ± 8.81	n.s.
R_{02}	0	4.40 ± 0.75	< 0.01
R_{42}	16.0 ± 1.34	6.99 ± 1.40	< 0.01
R_{24}	24.3 ± 8.14	(12.1)[c]	
R_{32}	8.32 ± 1.02	0.67 ± 0.49	< 0.01
R_{43}	8.32 ± 2.77	0.67 ± 4.43	< 0.05
R_{51}	0	0	
R_{52}	0	0	
R_{54}	6.08 ± 0.75	25.1 ± 4.36	< 0.01
R_{65}	1014	589	
R_{56}	1014	589	
R_{75}	233 ± 73.2	597 ± 222	< 0.05
$R_{05} + R_{75}$	926	930	

Transport rates of lipid-FA turnover between different lipid FA pools of the EFP, transport to plasma and oxidation to CO_2 were computed from the fractional rates (Table 1) and pool sizes (Table 2) (see text for details of computations).

[a] Same convention used for R_{ij} as that for L_{ij}, as defined in footnote to Table 1.

[b] Mean ± SD.

[c] This rate was calculated from the requirement of maintaining the pool size of cell-FFA at steady-state during our study.

amount of labeled ECF-FFA enters the circulation without first having been converted to TGFA in the adipocytes.

Our interpretations are strengthened by the following arguments. We considered the possibility that tracer in the injected bolus could not reach the systemic circulation because of reduced blood flow to the injected region. The possibility of tracer transport from ECF to a rather stagnant pool of blood within the fat pad was ruled out in two ways. First, after bolus injections of ^3H_2O and [^{14}C]glucose under the same conditions used to measure FFA transport in the present study, labels disappeared from the fat pad with a $t_{1/2}$ of a few minutes (Baker, N., V. Hill, and K. R. Bruckdorfer, unpublished observations). Second, in our present studies, the labeled FA disappearing from the ECF-FFA compartment was totally accounted for in cell-DGFA and cell-TGFA in fed mice. Both of these findings preclude the possibility of transport from the ECF-FFA (bolus region) into a stagnant pool of blood within the fat pad. Furthermore, even though blood flow (ml/g wet weight) to the adipose tissue has been reported to increase with fasting (20), we did not observe any direct rapid transport between the ECF-FFA and the plasma-FFA compartments in our fasted mice.

Our findings may at first seem totally unexpected based upon conventional models, which usually depict ECF-FFA exchanging directly with the plasma-FFA compartment (3, 13, 14). However, structure–function studies of adipose tissue in mice have made it apparent that FFA injected directly into the adipose tissue ECF need to travel considerable distances across the adipocyte plasma membrane surface before reaching a capillary (6, 16), thereby increasing the chances of cellular uptake of extracellular-FFA before entry into the circulation. Moreover, Blanchette-Mackie and Scow (21) have presented evidence supporting their hypothesis that channels exist at the sites of capillary-adipocyte contact through which FFA could theoretically be transferred directly from the circulation to the adipocyte and vice versa. Again, this pathway would be expected to by-pass the ECF-FFA compartment that is labeled by the direct tracer injection technique. We cannot imply anything about the movement of FFA from the plasma-FFA to cell-TGFA from our data. Whether this movement takes place without entry and mixing of plasma-FFA into the ECF- and cell-FFA compartments that we have measured here remains to be verified experimentally. This could be done by injecting tracer FFA intravenously and measuring its disappearance from plasma and its appearance in ECF- and cell-FFA and in other fractions. Such experiments are of utmost importance in delineating the nature and mechanisms of bi-directional FFA transport between the circulation and adipose tissue.

We have surmised that the processes of cellular FFA uptake, esterification, and recycling (to FFA) that we are studying are aspects of an apparently "futile cycle" that is off the main pathway of FFA transport into adipose tissue from the circulation or of FFA transport in the reverse direction. Several earlier workers (22–25) have reported and discussed the existence of such cycles in adipose tissue. In particular, Brooks, Jonathan, and Newsholme (25) have suggested that these cycles are of considerable importance in increasing the sensitivity of enzymes to metabolic control.

If we are correct, then we are observing a number of very marked effects of fasting on this "idling cycle."[3] These effects, as well as other responses to fasting of adipose tissue (in this case, EFP of anesthetized mice, specifically observed in this study), can be summarized as follows.

a) Fractional rates of transport (Table 1) among the different EFP-lipid-FA compartments that comprise the cycle are decreased by fasting. In contrast, an irreversible loss from the cell-FFA compartment occurs in fasting

[3] It is highly unlikely that such active cycles of FFA esterification and hydrolysis are "futile," hence, the quotation marks. Prof. J. F. Mead (Laboratory of Biomedical and Environmental Sciences, UCLA) has suggested (personal communication) that a more useful term for this type of process involving metabolic fuels might be "idling cycle." He suggests, as have Brooks et al. (25), that the system may be able to respond more promptly to hormonal signals when it is idling, at the expense of wasted energy, than when it is operating at a zero rate in any particular direction and then is signalled to become highly active. The analogy to a gasoline engine's response to an influx of gasoline when it is idling compared to when it needs to be started from the off condition, and the benefits and disadvantages (wasted fuel) are apparent. Subsequently, the term "idling turnover" has been applied independently to an enzyme system by Misrahi, Benkovic, and Benkovic (26).

(L_{02} = 0.017 min^{-1}) that is absent in the fed state. In addition, the following fractional rates are increased by fasting (as compared to the fed state): transport of hydrolyzed cell-TGFA into plasma-FFA (L_{54}), fivefold; plasma-FFA oxidation (L_{75}), twofold; and the portion of the total plasma-FFA irreversible disposal that is due to oxidation [$L_{75}/(L_{05} + L_{75})$], from 1/4 in the fed to ≃2/3 in the fasted mice. The transport rates (nmol FA/min) of hydrolyzed cell-TGFA to plasma-FFA (R_{54}) and of plasma-FFA oxidation to CO_2 (R_{75}) are increased by fasting, 4.1- and 2.6-fold, respectively (Table 3).

b) There is a moderate (≃30%) but significant increase in the pool size of ECF-FFA; however, the measured cell-FFA pool size increases by more than a factor of two (Table 2). There is also a moderate but significant decrease (≃25%) in the measured total TGFA pool size during fasting. On the other hand, the plasma-FFA pool size does not change significantly after a fasting period of 48 hr. The latter finding seems surprising, since fasting is known to increase both the mobilization of FFA from adipose tissue and plasma-FFA levels (13, 27, 28, 29). However, in another study, we have again observed that plasma-FFA levels of mice fed ad libitum, studied in the late morning, were not significantly different from those fasted for 48 hr (Baker, N., M. Elepano, and J. F. Mead, unpublished observations). In the latter experiments, a significant increase in plasma-FFA levels occurred between very early and late morning, as well as between very early morning and briefly fasted (4 hr postabsorptive), levels. Thus, the animals fed ad libitum in the present study were probably in the "early postabsorptive state" (30) at which time plasma-FFA levels reach a maximum and fail to increase during a subsequent 48-hr fasting period.

c) As an expression of the inherent nonhomogeneities of the cell-FFA and cell-TGFA pools, only a fraction of the measured values of these pools was estimated to be involved in the "idling cycle" in our short-term kinetic studies (i.e., ≃20-35% of the measured cell-FFA pool and ≃20–35% of the measured cell-FFA pool and ≃0.2% of the measured cell-TGFA pool (Table 2). The changes in the computed pool sizes in response to fasting were in the same direction as the changes in the measured pool sizes, but the magnitudes of the computed changes versus the measured ones were quite different.

d) Using the measured ECF-FFA and plasma-FFA pool sizes and the pool sizes computed from steady-state assumptions, six of the estimated FA transport rates were altered significantly by fasting (Table 3). While turnover of FFA (nmol FA/min) between the ECF- and cell-FFA compartments does not seem to change significantly during fasting, the total esterification rate of cell-FFA to cell-TGFA (i.e., $R_{42} + R_{32}$) drops significantly (by ≃70%).

Thus, fasting inhibits the putative "idling cycle" that is measured with the present tracer technique. It is well-established that fasting raises the rate of FFA mobilization from adipose tissue (e.g., 13, 28, 29). On the other hand, when TGFA is being synthesized and stored, the "idling cycle" of esterification and hydrolysis is increased markedly. Whether there is any interaction between these two inversely correlated processes (the cycle and net movement of FFA into and out of adipocytes) is not known; however, the possible relationship deserves further detailed study.

The significance of these "idling cycles" to the organism and how they are modified in abnormal physiological states in which fat is either lost or accumulated excessively remains to be determined. The cycle has been shown to be impaired markedly in the epididymal fat pads of mice bearing Ehrlich ascites carcinoma, a situation in which the fat pad is bathed by the tumor fluid and is invaded by the cancer cells. It is worth noting that the cycle can be impaired without an appreciable loss of adipose tissue-TGFA from the fat pads of tumor-bearing mice (7, 16).

Two other aspects of our study deserve special comment. First, we were unable to account for a very large fraction of the labeled FFA that disappeared from the EFP of fasted mice. It did not appear as expired $^{14}CO_2$ in the course of the experiment, and it did not appear as lipids in the circulation. One possibility is that the fat pads of fasted mice are especially leaky; however, this seems highly unlikely in view of the low amount of radioactivity remaining in the ECF-FFA compartment (from which leakage is most likely to occur) at 5 min and the high recoveries of TLFA at that time in fed and fasted mice. Another possibility is that the FFA is converted to a highly polar or bound form that was not readily extractable with the solvents used. If so, this would represent a major metabolic fate for FFA in the fat pad of fasted mice. Analytical error seems highly unlikely in the light of the excellent recoveries at early times in both the fed and fasted mice. Second, there has been much attention given to the question of metabolic heterogeneity of tissue-FFA compartments (1–4); we are apparently dealing with one set of compartments (ECF-FFA and cell-associated FFA) that lie off the main pathway of FFA transport from adipose tissue to plasma. The integration of the present findings into the total picture of adipose tissue fat metabolism remains a challenging problem.

We thankfully acknowledge the excellent technical assistance of Ms. Brenda Guthrie and the expert secretarial assistance of Ms. Anita Starlight in preparation of the manuscript. This work was supported by NIH-USPHS Grant CA-15813 and Veterans Administration Research. Intramural computing funds were supplied by the School of Medicine, UCLA. Modeling was conducted using the SAAM (11) program on the IBM 3033 computer at the Office of Academic Computing, UCLA.

Manuscript received 10 March 1986 and in revised form 14 October 1986.

REFERENCES

1. Kerpel, S., E. Shafrir, and B. Shapiro. 1961. Mechanism of fatty acid assimilation in adipose tissue. *Biochim. Biophys. Acta.* **46:** 495–504.
2. Steinberg, D. 1964. Synthesis and breakdown of triglycerides in adipose tissue. *In* Fat as a Tissue. K. Rodahl and B. Issekutz, editors. McGraw-Hill Book Co., New York. 127–184.
3. Zierler, K. L., E. Rogus, G. A. Klassen, and D. Rabinowitz. 1965. Flux of palmitic acid across the adipose tissue membrane. *Ann. N.Y. Acad. Sci.* **131:** 78–90.
4. Henderson, R. J., W. W. Christie, and J. H. Moore. 1979. Esterification of exogenous and endogenous fatty acid by rat adipocytes in vitro. *Biochim. Biophys. Acta.* **573:** 12–22.
5. Heindel, J. J., S. W. Cushman, and B. Jeanrenaud. 1974. Cell-associated fatty acid levels and energy-requiring processes in mouse adipocytes. *Am. J. Physiol.* **226:** 16–24.
6. Baker, N., V. Hill, M. Jacobson, and K. R. Bruckdorfer. 1984. Fatty acid metabolism in adipose tissue of aging mice after direct tracer injection into fat pads. *Mech. Ageing Dev.* **27:** 295–313.
7. Ookhtens, M., D. Monitisano, I. Lyon, and N. Baker. 1986. Inhibition of fatty acid incorporation into adipose tissue triglycerides in Ehrlich ascites tumor-bearing mice. *Cancer Res.* **46:** 633–638.
8. Bligh, E. G., and W. J. Dyer. 1959. A rapid method of total lipid extraction and purification. *Can. J. Biochem. Physiol.* **37:** 911–917.
9. Hron, W. T., and L. A. Menahan. 1981. A sensitive method for the determination of free fatty acids in plasma. *J. Lipid Res.* **22:** 377–381.
10. Ookhtens, M., and N. Baker. 1979. Evaluation of impaired triglyceride fatty acid transport and oxidation for the detection of cancer in mice. *Cancer Res.* **39:** 5118–5123.
11. Berman, M., and M. F. Weiss. 1977. SAAM Manual. Washington, DC: GPO [DHEW Publication No. (National Institutes of Health) 76-730].
12. Baker, N., and V. Hill. 1982. The use of in vivo-in vitro labeling techniques to study phospholipid fatty acid turnover and fatty acid esterification into triglycerides in adipose tissue of aging mice. *Mech. Ageing Dev.* **19:** 343–359.
13. Baker, N., V. A. Hill, and M. Ookhtens. 1978. Regulation of plasma free fatty acid mobilization by dietary glucose in Ehrlich ascites tumor-bearing mice. *Cancer Res.* **38:** 2372–2377.
14. Baker, N., and M. C. Schotz. 1967. Quantitative aspects of free fatty acid metabolism in the fasted rat. *J. Lipid Res.* **8:** 646–660.
15. Stein, Y., and O. Stein. 1962. Metabolic activity of rat epididymal fat pad labeled selectively by an in vivo incubation technique. *Biochim. Biophys. Acta.* **54:** 555–571.
16. Baker, N. 1985. In vivo tracer studies of perturbed fatty acid transport and metabolism in adipose tissue. *Int. J. Obes.* **9, Suppl. 1:** 155–167.
17. Ookhtens, M., and N. Baker. 1982. Essential and nonessential fatty acid oxidation in mice bearing Ehrlich ascites carcinoma. *Lipids.* **17:** 65–71.
18. Vaughn, M., D. Steinberg, and R. Pittman. 1964. On the interpretation of studies measuring uptake and esterification of [1-^{14}C]palmitic acid by rat adipose tissue in vitro. *Biochim. Biophys. Acta.* **84:** 154–166.
19. Ekstedt, B., and T. Olivecrona. 1970. Uptake and release of fatty acids by rat adipose tissue: last in–first out? *Lipids.* **5:** 858–860.
20. Mayerle, J. A., and R. J. Havel. 1969. Nutritional effects on blood flow in adipose tissue of unanesthetized rats. *Am. J. Physiol.* **217:** 1694–1698.
21. Blanchette-Mackie, E. J., and R. O. Scow. 1981. Membrane continuities within cells and intercellular contacts in white adipose tissue of young rats. *J. Ultrastruct. Res.* **77:** 277–294.
22. Ball, E. G., and R. L. Jungas. 1961. On the action of hormones which accelerate the rate of oxygen consumption and fatty acid release in adipose tissue in vitro. *Proc. Natl. Acad. Sci. USA.* **47:** 932–940.
23. Ball, E. G., and R. L. Jungas. 1964. Some effects of hormones on the metabolism of adipose tissue. *Recent Prog. Horm. Res.* **20:** 183–214.
24. Vaughan, M. 1962. The production and release of glycerol by adipose tissue incubated in vitro. *J. Biol. Chem.* **237:** 3354–3358.
25. Brooks, B., R. S. Jonathan, and E. A. Newsholme. 1982. Effect of hormones on the rate of the triacylglycerol/fatty acid substrate cycle adipocytes and epididymal fat pads. *FEBS Lett.* **146:** 327–330.
26. Mizrahi, V., P. A. Benkovic, and S. J. Benkovic. 1986. Mechanism of the idling-turnover reaction of the large (Klenow) fragment of *Escherichia coli* DNA polymerase I. *Proc. Natl. Acad. Sci. USA.* **83:** 231–235.
27. Waterhouse, C., N. Baker, and H. J. Rostami. 1969. Effect of glucose ingestion on the metabolism of free fatty acids in human subjects. *J. Lipid Res.* **10:** 487–494.
28. Baker, N., and H. J. Rostami. 1969. Effect of glucose feeding on net transport of plasma free fatty acids. *J. Lipid Res.* **10:** 83–90.
29. Dole, V. P. 1956. A relation between non-esterified fatty acids in plasma and the metabolism of glucose. *J. Clin. Invest.* **35:** 150–154.
30. Baker, N., D. B. Learn, and K. R. Bruckdorfer. 1978. Re-evaluation of lipogenesis from dietary glucose carbon in liver and carcass of mice. *J. Lipid Res.* **19:** 879–893.